Chinese Chemical Letters 34 (2023) 107707

Contents lists available at ScienceDirect

Chinese Chemical Letters

journal homepage: www.elsevier.com/locate/cclet

Electrochemical removal and recovery of phosphorus from wastewater using cathodic membrane filtration reactor

Lehui Ren, Jun Xu, Ruobin Dai*, Zhiwei Wang*

State Key Laboratory of Pollution Control and Resource Reuse, Advanced Membrane Technology Center of Tongji University, Shanghai Institute of Pollution Control and Ecological Security, School of Environmental Science and Engineering, Tongji University, Shanghai 200092, China

ARTICLE INFO

Article history:
Received 7 May 2022
Revised 20 June 2022
Accepted 22 July 2022
Available online 25 July 2022

Keywords:
Phosphate removal
Electrochemical precipitation
Cathodic membrane filtration
Enhanced mass transfer
Calcium phosphate

ABSTRACT

Removal and recovery of phosphorus (P) from wastewater is of great importance to addressing the challenges of eutrophication and phosphorus shortage. The P removal and recovery performance of conventional electrochemical precipitation approach was constrained by the limited mass transfer rate. Herein, a cathodic membrane filtration (CMF) reactor was developed using Ti/SnO_2-Sb anode and titanium mesh cathodic membrane module to achieve efficient removal and recovery of P in wastewater. Compared with the flow-by mode, the CMF system in the flow-through mode exhibited excellent P removal performance due to the markedly enhanced mass transfer. At the current density of 4 A/m^2, membrane flux of 16.6 L m^{-2} h^{-1}, and Ca/P molar ratio of 1.67, the removal efficiency of P was 96.2% and the energy consumption was only 45.7 kWh/kg P. The local high pH of cathode surface played a vital role in P removal, which substantially accelerated the nucleation of calcium phosphate (CaP). Based on the crystalline and morphological characterization of the precipitates, the hydroxyapatite was the most stable crystalline phase of CaP, which was transformed from intermediate phases (such as dicalcium phosphate and amorphous calcium phosphate). This study paves the way for applying electrochemical membrane filtration system for P removal and recovery from wastewater.

As one of the essential nutrients for living organisms, phosphorus (P) has been increasingly used in the production of daily necessities (such as fertilizers, food additives and detergent) with the growth of the global population [1,2]. However, as P is a non-renewable resource, its overexploitation has led to a gradual reduction in global P reserves [3]. It has been reported that, in 2015, the global phosphate rock production was 223,000 tons, while the remaining reserves were approximately 69 million tons [4]. Meanwhile, the excessive discharge of P in wastewater can induce the eutrophication of aquatic environment, which eventually leads to the hypoxia of aquatic organisms and the elimination of fish habitats [5,6]. Therefore, effective removal and recovery of P from wastewater is highly desirable to alleviate P resource shortage and facilitate environmental protection.

Various methods have been proposed for P removal in recent decades, including biological phosphorus removal [7], adsorption [8], and chemical precipitation [9,10]. The P-rich biomass resulting from biological phosphorus removal can possibly be used as agricultural fertilizer and other energy sources. However, the utilization of the P-rich biomass is still challenging due to the potential residues of pathogens, heavy metals, and other toxic compounds [11,12]. Although adsorption and chemical precipitation have been widely applied to recover phosphate from waste streams, large amounts of foreign ions and chemicals are simultaneously consumed [13,14]. Overall, the traditional P removal and recovery technologies still require further improvement to simplify operation procedure and reduce costs.

Electrochemical mediated precipitation (EMP) technology has recently attracted extensive attention in the field of wastewater treatment and resource recovery due to its advantages of simple operation, high automation and no reagent addition [15–17]. For instance, Lei *et al.* developed a column-shaped electrochemical reactor to treat cheese wastewater with tubular stainless steel cathode and achieved the P removal rate of 1267 mg/d [18]. However, most existing EMP systems are operated at the batch mode, and their P removal efficacies are constrained by limited convective mass transfer rate of P to the electrode surface, resulting in a relatively low removal efficiency and long hydraulic retention time [19,20]. Considering that the membrane filtration process can drive the solution/solute to the membrane surface [21–23], we hypothesize that the combination of EMP and membrane filtration tech-

* Corresponding authors.
E-mail addresses: dairuobin@tongji.edu.cn (R. Dai), zwwang@tongji.edu.cn (Z. Wang).

https://doi.org/10.1016/j.cclet.2022.07.050
1001-8417/

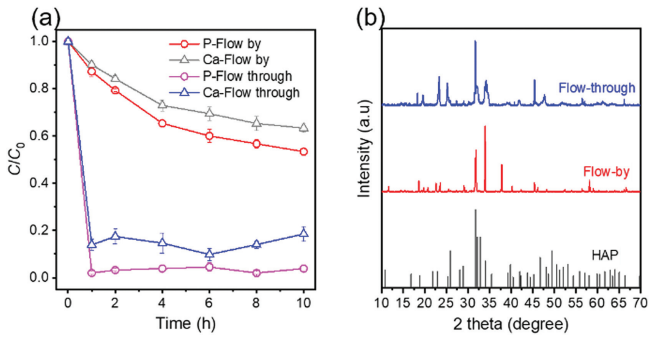

Fig. 1. (a) Comparison of the P and Ca removal and (b) XRD patterns of precipitates collected in the flow-by and flow-through modes. Experimental conditions: current density = 4 A/m^2, $[Ca^{2+}]_0 = 1.0$ mmol/L, $[PO_4\text{-}P]_0 = 0.6$ mmol/L, $Na_2SO_4 = 5$ mmol/L and pH 7.0.

nology can enhance the convective mass transfer rate and thereby improve P removal efficiency of the system.

Herein, a novel cathodic membrane filtration (CMF) reactor with Ti/SnO_2-Sb anode and porous titanium mesh cathode was developed for removal and recovery of P from wastewater (Fig. S1 in Supporting information). The removal performance of P in flow-by and flow-through modes was explored. The effects of different current density (0~1 A/m^2), membrane flux (0~22.1 L m^{-2} h^{-1}), and Ca/P molar ratio (1~7.5) on P removal in flow-through mode were investigated, and the mechanism of P precipitation in CMF system was proposed. The energy consumption of P removal and environmental application prospect of the system were evaluated. This study highlights the potential of applying electrochemical membrane filtration system for efficient P removal and recovery from wastewater.

The removal performance of P and Ca in the CMF system under the flow-by and flow-through modes was first evaluated (Fig. 1a). As expected, the flow-through mode exhibited superior P and Ca removal efficiency compared with the flow-by mode under the same current density. For instance, the P and Ca removal efficiencies after 10 h of electrolysis process at 4 A/m^2 were only 46.7% and 36.7% in the flow-by mode, respectively. In contrast, the P and Ca removal efficiencies were as high as 96.2% and 81.5% in the flow-through mode, respectively. This phenomenon could be attributed to the enhancement of convective mass transfer rate of solutes toward the cathodic membrane in the flow-through mode [24]. The transfer rate constant (k_m) (Fig. S2 in Supporting information) of the CMF system under two operation modes further verified that membrane filtration enhances the mass transport of P and Ca ions from the bulk solution to the cathode membrane surface. The crystal structures of collected solid precipitates under different operating modes were further characterized by X-Ray diffraction (XRD) (Fig. 1b). The XRD spectra showed that the precipitates formed in flow-by and flow-through modes have multiple identical diffraction peaks, which was well matched with the four peaks of commercial hydroxyapatite (HAP) in the range of 30°~35° [25]. These results indicated that the precipitates formed at the current operational condition in flow-by and flow-through modes were mainly HAP.

The effect of different operating conditions on P removal performance of the CMF system in the flow-through mode was further investigated. The effect of current density (Figs. 2a and b) on electrochemical removal of P and Ca was studied at the applied current density of 0, 2, 4, 8, and 16 A/m^2, respectively. When the current density was 2 A/m^2, the formation rate of OH^- was low. With the extension of electrolysis time, OH^- would be gradually consumed, resulting in the decrease in removal efficiency. After 10 h of electrolysis process, the removal efficiencies of P and Ca were increased from 68.2% and 36.7% to 96.2% and 81.5%, respectively, when the current density was changed from 2 A/m^2 to 4 A/m^2. This should be attributed to more OH^- produced near the cathode membrane surface by cathodic electroreduction of H_2O with the increase of current density. Local pH near the cathode (Fig. S3 in Supporting information) further validated that pH value increased with the increase of current density to a certain extent. Besides, the increased current density might enhance diffusion of Ca^{2+} to the cathode membrane surface [26], thereby improving the removal efficiency of P and Ca. However, the removal efficiencies of P and Ca had no obvious change when the current density was increased from 4 A/m^2 to 16 A/m^2. This phenomenon could be attributed to the concentrations of P and Ca ions rather than the current density, since the concentrations should have a great impact on the formation of calcium phosphate (CaP) precipitates [27].

The recovered products under different current density were further characterized. XRD patterns (Fig. 2c) showed that different crystalline products were produced with the increase of current density. When the current density was 2 A/m^2, the CaP solids were confirmed to be mainly dicalcium phosphate dihydrate ($CaHPO_4{\cdot}2H_2O$, DCPD), with characteristic diffraction peak at 11.6°. Despite the characteristic diffraction peaks belonging to HAP were observed at 30°~35°, the diffraction peak intensity was significantly lower than that of DCPD. However, when the current densities were 4, 8, and 16 A/m^2, the XRD diffraction peaks matched well with HAP. This tendency implied that the product of CaP recovery could be manipulated by the change in current density in future real applications. Furthermore, Raman spectrum (Fig. 2d) showed that the characteristic vibration of $\nu_1(PO_4^{3-})$ stretching occurred at 961 cm^{-1} at the applied current densities of 4, 8, and 16 A/m^2, which was the main scattering peak of HAP [28]. These results clearly demonstrated the formation of HAP at current densities of 4, 8, and 16 A/m^2. The composition of the recovered product was further supported by scanning electron microscope (SEM) images (Fig. 2e) and energy dispersive spectrometer (EDS) (Table S1 in Supporting information). When the current density was 2 A/m^2, the CaP solids showed a sheet shape, which was consistent with the reported morphology of DCPD [29,30]. However, when the current densities were 4, 8, 16 A/m^2, the CaP solids possessed a needle-like shape, which was the typical morphology of HAP. Simultaneously, a few spherical particles was observed, which was the typical morphology of amorphous calcium phosphate ($Ca_3(PO_4)_2$, ACP) [26]. This result indicated that the CaP solids formed were mainly HAP and contained a small amount of ACP.

The effects of different membrane flux (J = 0~22.1 L m^{-2} h^{-1}) on electrochemical removal of P was further investigated in the flow-through mode (Figs. 3a and b). It could be found that the CMF system exhibited high P removal efficiencies (>95%) under the membrane flux of 13.3 and 16.6 L m^{-2} h^{-1}. However, the further increase of membrane flux led to the decrease of P removal efficiency, because higher membrane flux might reduce the residence time of target pollutants (such as $H_2PO_4^-$, Ca^{2+}) at the vicinity of the membrane surface. The CaP precipitates therefore cannot form near the cathode surface and were discharged with the outflow. Another possible explanation was that the reaction rate with P and Ca ions decreased due to the accelerated discharge of OH^- on the cathode surface by membrane filtration [31]. Furthermore, the transmembrane pressure (TMP) at different membrane fluxes (J = 13.3, 16.6, 22.1 L m^{-2} h^{-1}) was monitored to evaluate the operation of the CMF system (Fig. S4 in Supporting information). The results showed that TMP under different membrane flux was maintained at a low level during 10 h operation, indicating that the CMF system had good stability and highlighting the potential of CMF system to remove and recover P in waste streams.

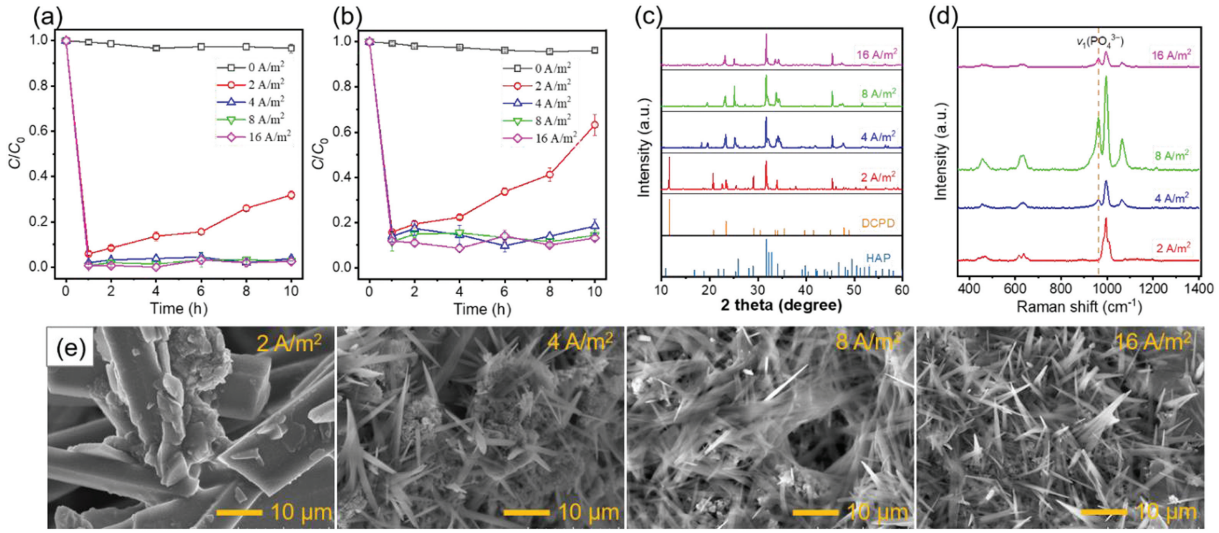

Fig. 2. Effect of current density on the removal of (a) P and (b) Ca, (c) XRD pattern and (d) Raman spectra of precipitates collected at different current density, and (e) SEM images of collected precipitates with different current density. Experimental conditions: current density = 0, 2, 4, 8, 16 A/m^2, J = 16.6 L m^{-2} h^{-1}, $[Ca^{2+}]_0$ = 1.0 mmol/L, $[PO_4\text{-}P]_0$ = 0.6 mmol/L, Na_2SO_4 = 5 mmol/L and pH 7.0.

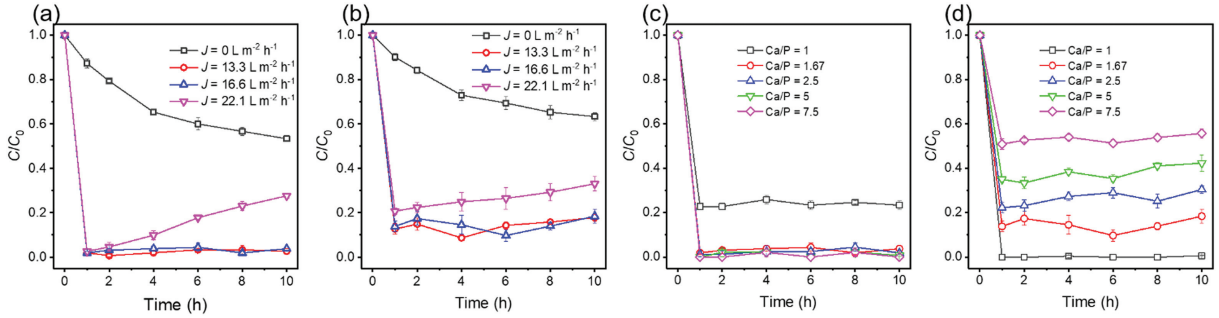

Fig. 3. Effects of (a, b) membrane flux and (c, d) Ca/P molar ratio on the removal of P and Ca. In plot a and b, current density = 4 A/m^2, J = 0, 13.3, 16.6, 22.1 L m^{-2} h^{-1}, $[Ca^{2+}]_0$ = 1.0 mmol/L, $[PO_4\text{-}P]_0$ = 0.6 mmol/L, Na_2SO_4 = 5 mmol/L and pH 7.0; In plot c and d, current density = 4 A/m^2, J = 16.6 L m^{-2} h^{-1}), $[PO_4\text{-}P]_0$ = 0.6 mmol/L, $[Ca^{2+}]_0$ = 0.6–1.5 mmol/L (Ca/P = 1, 1.67, 2.5) or $[PO_4\text{-}P]_0$ = 0.2 mmol/L, $[Ca^{2+}]_0$ = 1.0–1.5 mmol/L Ca^{2+} (Ca/P = 5, 7.5), 5 mmol/L Na_2SO_4, Na_2SO_4 = 5 mmol/L and pH 7.0.

Further experiments were conducted to investigate the effect of Ca/P molar ratio on electrochemical removal of P. As shown in Figs. 3c and d, after 10 h of electrolysis process, the removal efficiency of P increased from 76.1% to 96.8% when the Ca/P molar ratio increased from 1 to 1.67. The reason might be that the theoretical highest Ca/P molar ratio was 1.67 (HAP) in CaP precipitates [32], the driving force of CaP precipitates near the cathode membrane increased with the increase of Ca concentration in the solution [33]. However, the removal efficiency of P did not change significantly with the further increase of Ca/P molar ratio from 1.67 to 7.5. Moreover, it was found that the removal of Ca decreased from 81.5% to 44.2%, indicating that P concentration was the limiting factor for P removal.

The electrochemical mediated precipitation of P is generally ascribed to the local high pH value of the cathode surface, while phosphate ions do not directly participate in the electrochemical reaction [25]. Cyclic voltammetry (CV) scanning analysis was performed to investigate whether other reactions occurred during electrolysis. CV analysis results (Fig. S5 in Supporting information) showed that there was no additional peak at the Ti/SnO_2-Sb anode and titanium mesh cathode, indicating that only oxygen evolution reaction and hydrogen evolution reaction occurred on the anode and cathode surface, respectively. On the cathode surface, water molecules were reduced into H_2 and OH^- (Eq. 1). Dihydrogen phosphate ($H_2PO_4^-$) further reacted with OH^- to monohydrogen phosphate (HPO_4^{2-}) or phosphate (PO_4^{3-}) at the vicinity of the cathode membrane (Eqs. 2 and 3). Meanwhile, Ca^{2+} and phosphate would move towards and accumulate near the cathode due to the membrane filtration enhanced convective mass transfer and electromigration (Fig. 4a). Moreover, the thermodynamic driving force increased and the solubility of calcium phosphate decreased under the local high pH of cathode membrane, which significantly accelerated the nucleation and growth of calcium phosphate on the cathode surface. HAP is the most stable crystalline phase during the formation and precipitation of calcium phosphate. However, according to the relevant literature [27,34], the formation of HAP was much slower than that of DCPD and ACP in the terms of precipitation kinetics, and it depended on pH and electrolysis time in the terms of thermodynamics. Therefore, in the CMF system, DCPD was first formed, and then DCPD was converted to ACP or HAP, while ACP was also converted to HAP (Eqs. 4-7). The formed CaP precipitates were attached on the cathodic membrane surface through electrostatic interaction and continued to growing. Meantime, the CaP precipitates covering the cathodic membrane surface continuously fall to the bottom of the reactor due to the formation of hydrogen bubbles on the cathode surface.

$$2H_2O + 2e^- \rightarrow 2OH^- + H_2 \uparrow \quad (1)$$

$$OH^- + H_2PO_4^- \rightarrow HPO_4^{2-} + H_2O \quad (2)$$

$$OH^- + HPO_4^{2-} \rightarrow PO_4^{3-} + H_2O \quad (3)$$

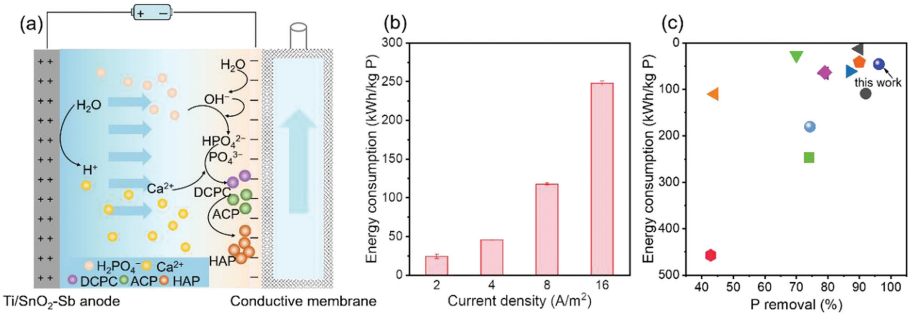

Fig. 4. (a) Schematic diagram of P removal mechanism in flow-through operated CMF system. (b) Electrical energy consumption for P removal at different applied current densities, (c) comparison of P removal rate and energy consumption with previously reported electrochemical systems (detailed information is summarized in Table S2 in Supporting information).

$$Ca^{2+} + HPO_4^{2-} + 2H_2O \rightarrow DCPD \downarrow \quad (4)$$

$$xCa^{2+} + yHPO_4^{2-}/PO_4^{3-} + nH_2O \rightarrow ACP \downarrow \quad (5)$$

$$DCPD + xCa^{2+} + yOH^- \rightarrow ACP \downarrow \quad (6)$$

$$DCPD/ACP + xCa^{2+} + yOH^- \rightarrow HAP \downarrow \quad (7)$$

Energy consumption is an important parameter to evaluate the economic feasibility of CMF system for P recovery. Fig. 4b shows the energy consumption for P removal at different current densities in flow-through mode. The energy consumption of CMF system increased with the increase of current density. When the current density was higher than 4 A/m^2, the energy consumption increased significantly, while the improvement of P removal efficiency was not obvious. These results indicated that 4 A/m^2 was the optimal choice for CMF system to remove P. Moreover, based on the results of flow-through mode, the P removal efficiency and energy cost were compared with those in existing literature (Fig. 4c). Compared with the other electrochemical systems for P removal, such as two anodes (steel and MMO) and stainless-steel cathode (E = 180.3 kWh/kg P and P removal efficiency = 74.3%) [35], tubular-shaped stainless-steel cathode (E = 27.0∼65.2 kWh/kg P and P removal efficiency = 40%∼79%) [18], Pt-Ti anode and Ti cathode (E = 64.7 kWh/kg P and P removal efficiency = 92.7%) [28], the CMF system showed lower energy cost (45.7 kWh/kg P) and higher P removal efficiency (96.2%), when the current density was 4 A/m^2 and the membrane flux was 16.6 L m^{-2} h^{-1}. These results indicated that CMF system has great potential to recover P from P-containing wastewater at relatively low energy cost.

The CMF system enhanced mass transfer by combining membrane filtration with EMP process, and improved the removal efficiency of low concentration P (0.6 mmol/L). Though natural organic matter (NOM) and bicarbonate in general showed inhibiting effects on CaP precipitation in conventional chemical precipitation process, CMF system can overcome the negative effects of co-ions in the water matrix by generating OH^- at the vicinity of the cathode to increase local pH [20,26]. Furthermore, membrane filtration simplifies the operating conditions and shortens the residence time, which facilitates the reduction of energy consumption in practical applications. While the feasibility of the system in actual wastewater needs to be further studied in the future, it may provide potential solutions to some P-containing waste streams.

In summary, a CMF reactor using Ti/SnO_2-Sb anode and titanium mesh cathodic membrane module was developed for P removal. The CMF system exhibited effective electrochemical removal for P in flow-through mode. Compared with the flow-by mode, the CMF system in the flow-through mode exhibited superior P and Ca removal efficiency due to the enhanced mass transfer. Current density of 4 A/m^2, membrane flux 16.6 L m^{-2} h^{-1}, and Ca/P molar ratio 1.67 were determined as the optimal conditions of the system. The results indicated that the local high pH of the cathode membrane surface played a vital role in P removal. The formed calcium phosphate was mainly the most stable crystalline phase HAP transformed from intermediate phases (such as DCPD and ACP) according to the characterization and analysis of precipitates. Compared with the other electrochemical methods in existing research, the CMF system showed lower energy cost (45.7 kWh/kg P) and higher P removal efficiency (96.2%). This study paves the way for applying electrochemical membrane filtration system for P removal and recovery from wastewater.

Declaration of competing interest

The authors declare that they have no known competing financial interests or personal relationships that could have appeared to influence the work reported in this paper.

Acknowledgments

National Natural Science Foundation of China (Nos. 51925806 & 51838009) and the Shanghai Sailing Program (No. 22YF1450700) for the financial support of the work are acknowledged.

Supplementary materials

Supplementary material associated with this article can be found, in the online version, at doi:10.1016/j.cclet.2022.07.050.

References

[1] D. Cordell, J.O. Drangert, S. White, Glob. Environ. Change 19 (2009) 292–305.
[2] B.K. Mayer, L.A. Baker, T.H. Boyer, et al., Environ. Sci. Technol. 50 (2016) 6606–6620.
[3] Z. Bradford-Hartke, J. Lane, P. Lant, et al., Environ. Sci. Technol. 49 (2015) 8611–8622.
[4] L. Delgadillo-Velasco, V. Hernández-Montoya, M.A. Montes-Morán, et al., J. Clean. Prod. 242 (2020) 118564.
[5] B.E. Rittmann, B. Mayer, P. Westerhoff, et al., Chemosphere 84 (2011) 846–853.
[6] W. Liu, P. Ciais, X. Liu, et al., Environ. Sci. Technol. 54 (2020) 14761–14771.
[7] S. Sun, M. Gao, Y. Wang, et al., Bioresour. Technol. 326 (2021) 124728.
[8] C. Li, H. Yu, S. Tabassum, et al., Chem. Eng. J. 331 (2018) 462–470.
[9] S. Ghosh, S. Lobanov, V.K. Lo, Environ. Sci. Pollut. Res. 26 (2019) 19063–19077.
[10] D. Guo, S. You, F. Li, et al., Chin. Chem. Lett. 33 (2022) 1–10.
[11] Y. Ye, H.H. Ngo, W. Guo, et al., Bioresour. Technol. 218 (2016) 874–881.
[12] Á. Robles, D. Aguado, R. Barat, et al., Bioresour. Technol. 300 (2020) 122673.
[13] L. Egle, H. Rechberger, J. Krampe, et al., Sci. Total Environ. 571 (2016) 522–542.
[14] Y. Ye, H.H. Ngo, W. Guo, et al., Sci. Total Environ. 576 (2017) 159–171.
[15] C. Kappel, K. Yasadi, H. Temmink, et al., Sep. Purif. Technol. 120 (2013) 437–444.
[16] C.A. Cid, J.T. Jasper, M.R. Hoffmann, A.C.S. Sustain, Chem. Eng. 6 (2018) 3135–3142.

[17] Y. Lei, J.C. Remmers, M. Saakes, et al., ACS Sustain. Chem. Eng. 7 (2019) 7362–7368.
[18] Y. Lei, Z. Zhan, M. Saakes, et al., Water Res. 199 (2021) 117199.
[19] Y. Lei, E. Geraets, M. Saakes, et al., Water Res. 169 (2020) 115207.
[20] Y. Lei, B. Song, M. Saakes, et al., Water Res. 142 (2018) 10–17.
[21] J. Zheng, J. Ma, Z. Wang, et al., Environ. Sci. Technol. 51 (2017) 2757–2765.
[22] L. Ren, M. Chen, J. Ma, et al., Chem. Eng. J. 428 (2022) 131194.
[23] D. Guo, Y. Liu, H. Ji, et al., Environ. Sci. Technol. 55 (2021) 4045–4053.
[24] C. Trellu, B.P. Chaplin, C. Coetsier, et al., Chemosphere 208 (2018) 159–175.
[25] Y. Lei, B. Song, R.D. van der Weijden, et al., Environ. Sci. Technol. 51 (2017) 11156–11164.
[26] Y. Lei, M. Saakes, R.D. van der Weijden, et al., Chem. Eng. J. 342 (2018) 350–356.
[27] Y. Lei, J.C. Remmers, M. Saakes, et al., Environ. Sci. Technol. 52 (2018) 8399–8407.
[28] Y. Lei, Z. Zhan, M. Saakes, et al., ACS EST Water 1 (2021) 1002–1013.
[29] G.R. Sivakumar, S. Narayana Kalkura, P. Ramasamy, Mater. Chem. Phys. 57 (1999) 238–243.
[30] L.I. Bowden, A.P. Jarvis, P.L. Younger, et al., Environ. Sci. Technol. 43 (2009) 2476–2481.
[31] J. Zheng, S. Xu, Z. Wu, et al., Sep. Purif. Technol. 211 (2019) 753–763.
[32] L. Wang, G.H. Nancollas, Chem. Rev. 108 (2008) 4628–4669.
[33] Y. Wang, P. Kuntke, M. Saakes, et al., Water Res. 209 (2022) 117891.
[34] B. Cichy, E. Kużdżał, H. Krztoń, J. Environ. Manage. 232 (2019) 421–427.
[35] S. Liang, W. Zheng, L. Zhu, et al., Environ. Sci. Technol. 53 (2019) 5328–5336.